Polynomial Chaos Analysis of Delay Effect on Uncertainties in Real-Time Hybrid Simulation

A Thesis submitted to the faculty of
San Francisco State University
In partial fulfillment of
the requirements for
the Degree

Master of Science

In

Engineering

by

Kai Chen

San Francisco, California

December 2016

CERTIFICATION OF APPROVAL

I certify that I have read Polynomial Chaos Analysis of Delay Effect on Uncertainties in Real-Time Hybrid Simulation by Kai Chen, and that in my opinion this work meets the criteria for approving a thesis submitted in partial fulfillment of the requirement for the degree Master of Science in Engineering: Structural Engineering & Earthquake Engineering at San Francisco State University.

Cheng Chen, Ph.D.
Associate Professor

Wenshen Pong, Ph.D.
Professor

Polynomial Chaos Analysis of Delay Effect on Uncertainties in Real-Time Hybrid Simulation

Kai Chen
San Francisco, California
2016

Uncertainties in numerical substructure can result in different responses for the same experimental substructure in hybrid simulation. This problem is more serious in real-time hybrid simulation when coupled with actuator delay. Polynomial chaos expansion (PCE) projects the model output on a basis of orthogonal stochastic polynomials, and provide an efficient and effective metamodel technique to represent the complex model. From the polynomial chaos expansion, the influence of the uncertainties in numerical model can be reflected. In this paper, PCE is utilized to evaluate the delay effect on the maximum structure responses when the numerical substructure contains uncertainties in real-time hybrid simulation.

I certify that the Abstract is a correct representation of the content of this thesis.

Chair, Thesis Committee

12/12/2016
Date

PREFACE AND/OR ACKNOWLEDGEMENTS

I express my sincere gratitude to my research adviser Prof. Cheng Chen, whose encouragement, guidance and support from the preliminary to the concluding part of my research enabled me to develop an understanding of the subject. Besides my advisor, I would like to thank the other member of my thesis committee Prof. Wenshen Pong.

I also wish to convey heartfelt thanks to my family and friends for their help, encouragement and moral support during the course of my project work.

Finally, and most importantly, I really thank my parents whom are always supporting me and encouraging me during my life. To them I dedicate my thesis.

TABLE OF CONTENTS

LIST OF TABLES

LIST OF FIGURES

Figures Page

CHARPTER I:

INTRODUCTION

1.1 UNCERTAINTY QUALIFICATION

Identifying the uncertainty sources can facilitate any attempt at reducing uncertainty [Liu, 2013]. It is however more interesting and useful to understand how the uncertainty can propagate through the model representation, such as algebraic equations, integral equations, differential equations or a combination of part of all of them, and impact the model outputs. This is often called uncertainty quantification which is the mathematical description of how the computational results are likely to possess certain (in the discrete case) values or to lie in a certain range of values (in the continuous case), in the presence of model uncertainty sources. A direct result of uncertainty in model outputs is that one can hardly rely on a single simulation of the model

Uncertainty quantification in large-scale simulations are play a more and more important role in the process of code verification and validation (V&V.) When the simulations have different results from the experiments, it is crucial to understand the expected uncertainty in the output metrics of the calculation and also have a quantitative determination of the error. It is possible to determine the true accuracy of a simulation when the uncertainty is less than the predicated uncertainty of the simulation.

1.2 MONTE CARLO METHOD

One method to study the uncertainty quantification called Monte Carlo method [Mooney, 1997]. The Monte Carlo method is considered to be the most robust way to study propagation of uncertainties and can be used for the quantification of uncertainty. A large

number of multi-dimensional sample points are drawn from the joint probability distribution characterizing the uncertainty sources, and model simulations are run at each of these sample points. The model solutions constitute a pool of model predictions under different sample values, whose average indicates the statistical moments of the model. The model being evaluated in a repetitive fashion is compared to a "black box", denoting the relationship between input and output. One does not need to understand what is going on inside the model, nor adjust the programming code. The non-intrusive feature of Monte Carlo methods renders itself suitable for parallel computing to deal with problems of large dimensions. However, the convergence rate of the Monte Carlo method is inversely proportional to the square root of the number of samples and directly proportional to the square root of the variance. To enhance the estimation accuracy, more sample points in the stochastic parameter space need to be generated and evaluated. This can hinder many applications where a large number of forward simulations are unaffordable due to limited resources [Liu, 2013].

Since the accuracy of this method highly depends on the sample size, the limited computational time and memory make simulation extremely expensive. To address this issue, variance reduction techniques are developed to increase the accuracy of the estimates by reducing the variability in the model outputs. Commonly used variance reduction methods include antithetic variates, control variates, importance sampling and stratified sampling [Rubinstein, 2007], Latin Hypercube sampling [Jon C., and Davis, 2013], Quasi-Monte Carlo method [Niederreiter and Harald, 2010]. One non-statistical methods are based on discretizing the random process in random space [Pettersson et al., 2015]. Karhunen-Loeve expansion utilizes a set of orthogonal functions and constant values determined by the spectral expansion of the correlation function to represent a random process [Huang and Quek, 2002]. This expansion has the smallest mean-square error resulting from a finite representation of the random process among other possible decompositions, which is also called error minimizing property. However, this method is not suitable when the covariance function is not known.

1.3 POLYNOMIAL CHAOS EXPANSION

Wiener [1938] developed the polynomial chaos expansion (PCE) technique to treat "Homogeneous Chaos", where a Gaussian process is represented by a series of Hermite polynomials. The polynomial chaos of order p is the p^{th} order polynomials in the random variables spanning the p^{th} homogeneous chaos. Karhunen and Loeve in 1947 and 1948 [Liu, 2013] separately proposed a Fourier-type series expansion for a random process which is named the Karhunen-Loeve (KL) expansion. The KL expansion expands a random process as an infinite linear combination of orthogonal functions with the product of eigenvalues and eigenvectors of the associated covariance function as the coefficients. The expansion is unique and optimal in the sense that the mean-square error of the KL expansion is minimized. However, the covariance function necessary to compute the expansion coefficients is generally not known for a model solution process. The orthogonal polynomials in the polynomial chaos expansion for a Gaussian process can be derived through an orthogonalization procedure and it turns out that they coincide with Hermite polynomials. Cameron and Martin [Ernst, 2011] showed that the expansion is convergent in the L2 norm for a stochastic process with finite variance. In fact, spectral accuracy can be achieved for a Gaussian process. Polynomial chaos can also be applied to a random process involving spatial and temporal variables. The expansion of such processes separates the spatiotemporal space and the random event space. For a non-Gaussian process, the polynomial chaos expansion can be constructed by projecting the process on the Hermite polynomial basis. The coefficients of the expansion are usually obtained by the normalized inner products of the process and the polynomials. The statistical moments can be obtained directly from the polynomial chaos expansion, due to the orthogonality of the expansion basis. It has also been observed that the convergence rate of polynomial chaos expansion in terms of Hermite polynomials is slower if the underlying process is non-Gaussian [Ernst et al., 2011]. Xiu and Karniadakis [2002] extended the original framework by introducing a variety of orthogonal polynomials from the Askey-scheme for the construction of polynomial chaos expansions. The weighting function of each of these orthogonal polynomials corresponds to the probability density function of a certain random

distribution. This extended chaos expansion achieves optimal accuracy, and is known as the generalized polynomial chaos expansion. Recently, Wan and Karniadakis [2005] developed a method which decomposes the random space into subspaces and builds generalized polynomial chaos in each subspace. This method generally enhances the performance of chaos expansion with global orthogonal basis, and is especially suitable for problems with discontinuities in stochastic space.

1.4 SENSITIVTY ANALYSIS

Sensitivity analysis is a technique used to determine how different values of an independent variable will impact a particular dependent variable under a given set of assumptions.

Crestaux and Thierry [2009] presented a method for the computation of the Sobol sensitivity indices of a function (or model output) involving independent random output, with known probability distributions. This method uses the PCE of the function to directly compute the conditional variances and sobol's sensitivity indices. The most important two points of this approach is:

1. The simple and immediate computation of the sensitivity indices from the Polynomial Chaos Expansion.

2. The different methods available for the determination of the PCE, such as Galerkin project, NISP and least square approximation.

The result shows that the convergence of the rates of the PCE and MC are almost the same and the PC method remains competitive to MC methods.

1.5 REAL-TIME HYBRID SIMULATION

Real□time hybrid simulation (RTHS) has increasingly been recognized as a powerful methodology to evaluate structural components and systems under realistic operating conditions. It is a cost effective approach compared with large scale shake table testing. Real-time hybrid testing combines experimental testing and numerical simulation, and provide a viable alternative for the dynamic testing of structural systems [Chen, 2009], which are simulated in computer and tested in laboratory respectively. The substructure technique reduces the testing cost and makes full scale test possible.

In real-time hybrid simulation, the restoring force of the experimental substructure is measured before the actuator reaches its target position. This lag is called time delay and would lead to inaccurate test results [Horiuchi et al, 1999]. Though the time delay is varying in test, conventional delay compensation methods compensate constant delay, such as polynomial extrapolation method and linear acceleration extrapolation [Horiuchi et al, 1999]. With the development of the control theory, methods based on constant actuator dynamics are also proposed, such as model-based prediction [Carrion et al., 2006] and inverse compensation method [Chen, 2008]. By introduce the concept of adaptive control, AIC (adaptive inverse compensation) method [Chen, 2009] which is based on the inverse compensation method and Feedforward-Feedback Tracking Control [Chen, 2010] based on model model-based compensation method have been proposed. These adaptive compensation methods can adjust parameters during the test, so that can compensate variable delay.

The experimental substructure in real-time hybrid simulation is exactly the same as the structure to be tested. However, the model for numerical substructure may not exactly the same as testing structure due to the lack of knowledge. It is difficult to measure the parameters of the structure exactly, which results in the uncertainties in numerical modeling. Besides, the structure properties may vary during the test, which are also difficult to model accurately. Thus, the real-time hybrid simulation should be regarded as a random process, which contains model uncertainties in numerical substructure. When consider delay effect, the propagation of the uncertainties to the output are rather complex.

CHARPTER II

POLYNOMIAL CHAOS EXPANSION

2.1 THE ORIGINAL POLYNOMIAL CHAOS EXPANSION

Polynomial Chaos Expansion (PCE) is a powerful metamodeling tool that has important applications in many engineering and applied mathematics fields such as structural reliability and sensitivity analysis. Due to the underlying complexity of its formulation, however, this technique has been relatively little use outside of these field.

The original PCE was also called Hermite Polynomial Chaos, introduced by Wiener in 1938. It makes Hermite Polynomials cooperate with Gaussian random variables. According to a theorem by Cameron and Martin, it can approximately any functionals in $L_2(C)$ and converges in the $L_2(C)$ sense. Therefore, Hermite-Chaos provides a means for expanding second – order random processes in terms of orthogonal polynomials. Second-order random processes are processes with finite variance, and this applies to most physical processes. Thus, a general second-order random process $X(\theta)$, viewed as a function of θ as the random event, can be represented in the form,

$$
\begin{aligned}
X(\theta) &= a_0 H_0 \\
&+\sum_{i_1=1}^{\infty} a_{i_1} H_1(\xi_{i_1}(\theta)) \\
&+\sum_{i_1=1}^{\infty}\sum_{i_2=1}^{i_1} a_{i_1 i_2} H_2(\xi_{i_1}(\theta),\xi_{i_2}(\theta)) \\
&+\sum_{i_1=1}^{\infty}\sum_{i_2=1}^{i_1}\sum_{i_3=1}^{i_2} a_{i_1 i_2 i_3} H_3(\xi_{i_1}(\theta),\xi_{i_2}(\theta),\xi_{i_3}(\theta)) \\
&+\cdots
\end{aligned}
\tag{2-1}
$$

where $H_n(\xi_{i_1} \cdots\cdots \xi_{i_n})$ denotes the Hermite-Chaos of order n in the variables $H_n(\xi_{i_1} \cdots\cdots \xi_{i_n})$, and H_n are Hermite polynomials in terms of the standard Gaussian variables ξ with zero mean and unit variance. Here ξ denotes the vector consisting of n independent Gaussian variables $H_n(\xi_{i_1} \cdots\cdots \xi_{i_n})$. Eq(2-1) is the discrete version of the original Wiener polynomial chaos expansion, where the continuous integrals are replaced by summations. The general expression of the polynomials is given by

$$H_n(\xi_{i_1} \cdots\cdots \xi_{i_n}) = e^{\frac{1}{2}\xi^T\xi}(-1)^n \frac{\partial^n}{\partial\xi_{i_1} \cdots\cdots \partial\xi_{i_n}} e^{\frac{1}{2}\xi^T\xi} \tag{2-2}$$

For notational convenience, Eq (2-2) can be rewritten as

$$X(\theta) = \sum_{j=0}^{\infty} \hat{a}_j \psi_j(\xi) \tag{2-3}$$

where there is a one – to –one correspondence between the functions $H_n(\xi_{i_1} \cdots\cdots \xi_{i_n}(\theta))$ and $\psi_j(\xi)$. The polynomial basis $\{\psi_j\}$ of Hermite-Chaos forms a complete orthogonal basis, i.e.,

$$\langle \psi_i \psi_j \rangle = \langle \psi_i^2 \rangle \delta_{ij} \tag{2-4}$$

where δ_{ij} is the Kronecher delta and $\langle \cdot, \cdot \rangle$ denotes the ensemble average. This is the inner product in the Hilbert space determined by the support of the Gaussian variables

$$\langle f(\xi)g(\xi) \rangle = \int f(\xi)g(\xi)W(\xi)d\xi \tag{2-5}$$

Where the weighting function is

$$W(\xi) = \frac{1}{\sqrt{(2\pi)^n}} e^{\frac{1}{2}\xi^T\xi} \tag{2-6}$$

What distinguishes the Hermite-Chaos expansion from other possible expansions is that the basis polynomials are Hermite polynomials in terms of Gaussian variables and are orthogonal with respect to the weighting function $W(\xi)$ that has the form of n-dimensional independent Gaussian probability density function.

2.2 THE WIENER – ASKEY POLYNOMIAL CHAOS EXPANSION

The Hermite-Chaos expansion has been proved to be effective in solving stochastic process with non-Gaussian inputs. However, for general non-Gaussian random inputs, the optimal exponential convergence rate will not be realized. To solve this problem, Askey-scheme is used to derivate the generalized polynomial chaos, it can be represented as:

$$\begin{aligned} X(\theta) &= a_0 H_0 \\ &+ \sum_{i_1=1}^{\infty} c_{i_1} I_1(\varsigma_{i_1}(\theta)) \\ &+ \sum_{i_1=1}^{\infty} \sum_{i_2=1}^{i_1} c_{i_1 i_2} I_2(\varsigma_{i_1}(\theta), \varsigma_{i_2}(\theta)) \\ &+ \sum_{i_1=1}^{\infty} \sum_{i_2=1}^{i_1} \sum_{i_3=1}^{i_2} c_{i_1 i_2 i_3} I_3(\varsigma_{i_1}(\theta), \varsigma_{i_2}(\theta), \varsigma_{i_3}(\theta)) \\ &+ \cdots \end{aligned} \tag{2-7}$$

where $I_n(\varsigma_{i_1} \cdots\cdots \varsigma_{i_n})$ denotes the Wiener-Askey polynomial chaos of order n in terms of the random vector $\varsigma = (\varsigma_{i_1} \cdots\cdots \varsigma_{i_n})$. In the Wiener-Askey chaos expansion, the polynomials I_n are not restricted to Hermite polynomials but rather can be all types of the orthogonal polynomials from the Askey-scheme in figure 3.1. Again for notational convenience, the equation:

$$X(\theta) = \sum_{j=0}^{\infty} \hat{c}_j \Phi_j(\varsigma) \tag{2-8}$$

where there is a one-to-one correspondence between the functions $I_n(\varsigma_{i_1} \cdots\cdots \varsigma_{i_n})$ .The orthogonal relation of the Wiener-Askey polynomial chaos takes the form

$$\langle \Phi_i \Phi_j \rangle = \langle \Phi_i^2 \rangle \delta_{ij} \tag{2-9}$$

where δ_{ij} is the Kronecher delta and $\langle \cdot, \cdot \rangle$ denotes the ensemble average. This is the inner product in the Hilbert space determined by the support of the variables ς

$$\langle f(\varsigma) g(\varsigma) \rangle = \int f(\varsigma) g(\varsigma) W(\varsigma) d\varsigma, \tag{2-10}$$

or

$$\langle f(\varsigma) g(\varsigma) \rangle = \sum_{\varsigma} f(\varsigma) g(\varsigma) W(\varsigma) \tag{2-11}$$

in the discrete case. Here $W(\varsigma)$ is the weighting function corresponding to the Wiener-Askey polynomials chaos basis $\{\Phi_i\}$.

The commonly used polynomials are presented in Table 2.1.

Tab. 2.1 commonly used polynomial chaos

Type of the random variable	Type of polynomials chaos
Uniform	Legendre
Gaussian	Hermite
Gamma	Laguerre
Beta	Jacobi

2.3 SOBOL INDEX

The convergence of the polynomial chaos expansion can be determined by the Sobol index. Sobol index is a global index used for estimating the influence of individual

variables or groups of variables on the model output [32]. The Sobol index can also be used to determine the accuracy of the polynomial chaos expansion, which compared with the Sobol index calculated by Monte Carlo simulation.

The integrable function

$$f(x) = f_0 + \sum_{s=1}^{n} \sum_{i_1<\cdots<i_s}^{n} f_{i_1\cdots i_s}(x_{i_1}, \cdots, x_{i_s}) \tag{2-12}$$

which defined in I^n is called ANOVA-representation of $f(x)$ if

$$\int_0^1 f_{i_1\cdots i_s}(x_{i_1}, \cdots, x_{i_s}) dx_k = 0 \quad (k = i_1, \cdots, i_s) \tag{2-13}$$

where f_0 is a constant value.

The ANOVA-representation is unique for $f(x)$, which each term can be derived by

$$f_i(x_i) = \int_{I^{n-1}} f(x) dx_{\sim i} - f_0 \tag{2-14}$$

$$f_{i,j}(x_i, x_j) = \int_{I^{n-2}} f(x) dx_{\sim ij} - f_0 - f_i(x_i) - f_j(x_j) \tag{2-15}$$

...

$dx_{\sim i}$ denotes the integration over all parameters except x_i.

Defining total variance D and partial variance D as

$$D = \int_I f^2(x) dx - f_0^2 \tag{2-16}$$

$$D_{i_1\cdots i_s} = \int_I f_{i_1\cdots i_s}{}^2(x_{i_1}, \cdots, x_{i_s}) dx_{i_1\cdots i_s} \tag{2-17}$$

Then, the Sobol index is defined as

$$S_{i_1\cdots i_s} = D_{i_1\cdots i_s} / D \tag{2-18}$$

where $S_{i_1 \cdots i_s}$ describes the influence of the input parameter on the amount of the total variance. It is clear that the range of the Sobol index varies from 0 to 1. The larger Sobol index is, the more influence of the parameter on the amount of total variance. However, the computational effort increase exponential with the input parameters, so only first order Sobol index and total Sobol index are mainly used in practice.

The first order Sobol index S_i (i=i_1, $i2$…) represents the influence of i-th input parameter alone on the total output variance. On the other hand, total Sobol index S_{Ti} represents the influence of i-th input parameter combined with other parameters on the total output variance.

2.4 UQLAB

The UQlab is a Matlab-based software framework for uncertainty quantification. It is a powerful tool to calculate the coefficients of the polynomial chaos and it can be classified as two types: projection method and regression method.

The process of Matlab solving uncertainty quantification problems can be simplified as below:

INPUT module: a joint PDF representing the uncertain input parameters.

MODEL module: a function that operates on samples extracted from the INPUT and calculates the corresponding model reponse.

ANALYSIS module: a reliability analysis associated with a failure criterion on the model response.

In this study, the Uqlab is used to calculate the mean and variance maximum displacement through the computational model with the mass, damping ratio and stiffness are random variables.

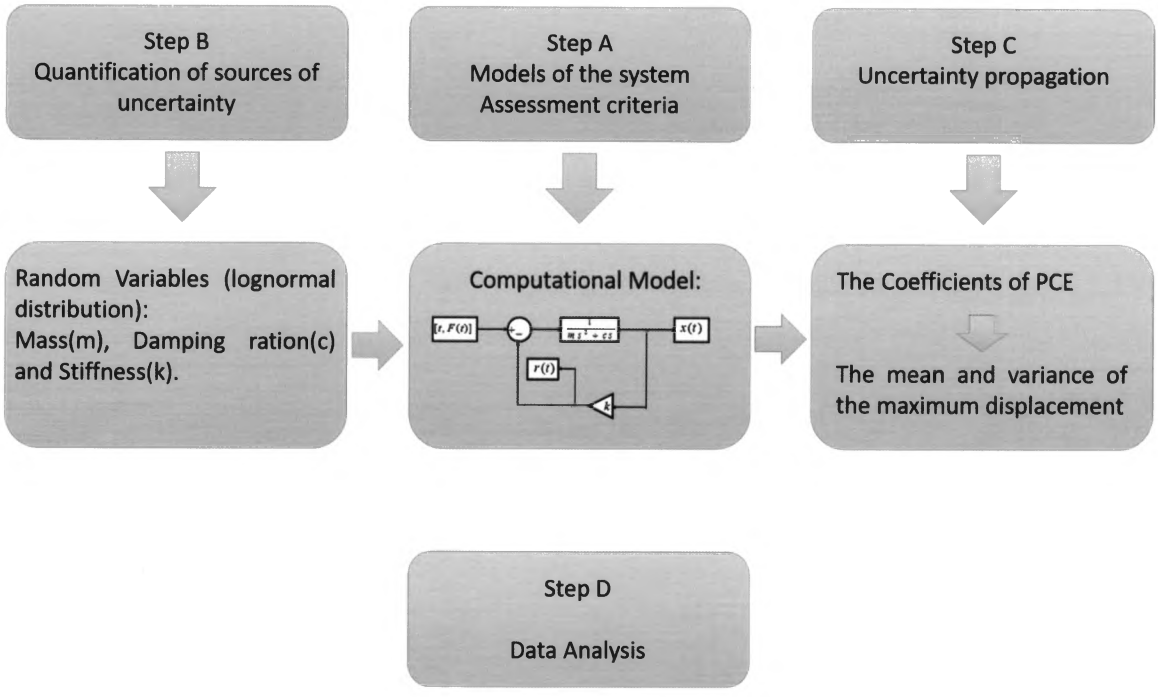

Figure 2-1 Flow Chart of the UQlab Analysis

CHARPTER III

DELAY EFFECT IN SINGLE-DEGREE-OF-FREEDOM (SDOF) SYSTEM

3.1 POLYNOMIAL CHAOS EXPANSION FOR SDOF SYSTEM WITHOUT DELAY

3.1.1 DDE MODEL FOR SDOF SYSTEM

Single-degree-of-freedom (SDOF) system is a system whose motion is defined just by a single independent co-ordinate (or function). SDOF systems are often used as a rough mode for a generally more complex system.

A typical SDOF mass-spring oscillator system shown in Figure 3-1.

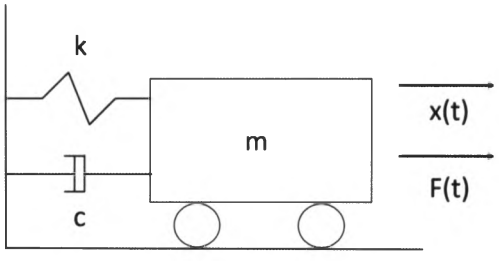

Figure 3-1 Typical SDOF mass- spring oscillator

In this study, the polynomial chaos is utilized to evaluate the delay effect on the maximum structural responses when numerical substructure contains uncertainty parameters in real-time hybrid simulation using delay differential equation (DDE) model.

DDEs are types of differential equation in which the derivative of the unknown function at a certain time is given in terms of the values of the functions at previous times. The DDE model is very useful to understand the influence of the delay on real-time hybrid simulation [Wallace et al., 2006]. The delay effect on model uncertainty is explored when DDE model built as stochastic system with undetermined parameters.

For simplicity but without loss of generality, the mass, damping and stiffness all follow lognormal distribution in DDE model. The mean values of the mass, damping and

stiffness are 1kg, 0.2513 and 39.4784KN/mm, respectively. The variances of the three variables are one in ten of their mean values. The MU2035 component recorded at Beverly Hills - Mulholstation during the 1994 Northridge earthquake is selected from the PEER Strong Motion Database with the peak ground acceleration of 0.617g. When the mean values of the random variables are selected, the maximum displacement of the response is 0.1007m.

The mass-spring oscillator with an excitation force input F(t) shown in Figure 3.1 can be expressed as:

$$m\cdot\ddot{x}(t)+c\cdot\dot{x}(t)+k\cdot x(t)=F(t) \tag{3-1}$$

where m, c, k are the mass viscous damping and stiffness of the SDOF structure, respectively; t is time function; $\dot{x}(t)$ and $\ddot{x}(t)$ are the velocity and acceleration responses of the SDOF structure, respectively; and $F(t)$ is the external excitation force.

It is assumed that in real-time hybrid simulation, all stiffness belongs to experimental substructure while all damping belongs to numerical substructure. So, the stiffness is isolated as experimental substructure while the rest of the SDOF structure is modeled as analytical substructure including the inertial mass and the viscous damping. When time delay exists in the response of servo-hydraulic actuator, the equation can be written as:

$$m\cdot\ddot{x}(t)+c\cdot\dot{x}(t)+k\cdot x(t-\tau)=F(t) \tag{3-2}$$

where τ is the time delay due to-hydraulic dynamics. Also, the Simulink model based on the DDE can be created as:

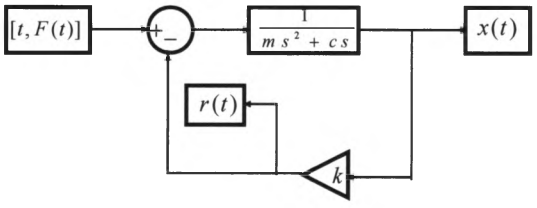

Figure.3-2 Simulink model of SDOF system with time delay

3.1.2 MONTE CARLO SIMULATION FOR SDOF SYSTEM

Before calculating polynomial chaos expansion, three problems should be determined: the method to calculate polynomial chaos, the order of the polynomial chaos expansion and the number of the sampling point. For this reason, 50000 Monte Carlo simulations are conducted to calculate the mean and variance of the maximum displacement as well as Sobol indexes for each parameter when mass, damping and stiffness are random variables. The results of the 50000 Monte Carlo simulations are considered as standard values for this DDE model.

The mean and variance of the maximum displacement calculated by 50000 Monte Carlo simulations are 0.1094 and 2.376×10^{-4}, respectively. The first order Sobol indices and total Sobol indices for each parameter are shown in Table .3.1.

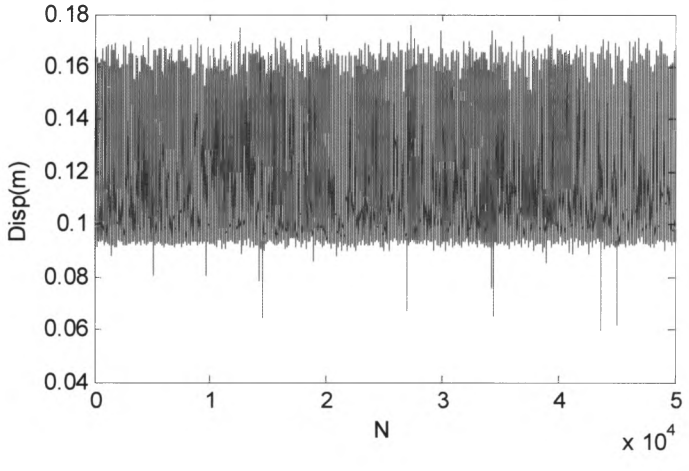

Figure. 3-3 Maximum displacements for each simulation

Tab. 2 Sobol indices of the random variables

	m	*c*	*k*
First order	0.4383	0.0108	0.2682
Total	0.7106	0.0180	0.6358

Compared with maximum displacement in no uncertainty case, the mean of the maximum displacements calculated by 50000 Monte Carlo simulations is 8.6% larger. In other words, the mean of the maximum displacement does not necessarily equal to the maximum displacement when random variables equal to their mean values. This leads to the need for uncertainty quantification when model contains random variables.

3.1.3 METHODS TO CALCULATE POLYNOMIAL CHAOS EXPANSION

As mentioned before, the approaches for coefficients determination can be classified as two types: intrusive and non-intrusive. For non-intrusive method, it may contain two methods, the projection method and regression method.

To compare the performance of projection method and regression method, first order, third order and eighth order polynomial chaos expansions are conducted using UQlab. The number of coefficients are 4, 20, 156 for first order, third order and eighth order polynomial chaos expansions when mass, damping and stiffness are random variables. In UQlab, the number of sample for projection method is determined by the software. The numbers of sample are 7, 83 and 2541 for first order, third order and eighth order polynomial chaos expansions respectively. On the other hand, the number of sample for regression method can be determined by researchers. For this reason, the same sample points for regression method are selected as projection method. The LARS method is used in regression, which only part of the coefficients is calculated. The coefficients calculated by the projection method and regression method shown in Figure 3-4.

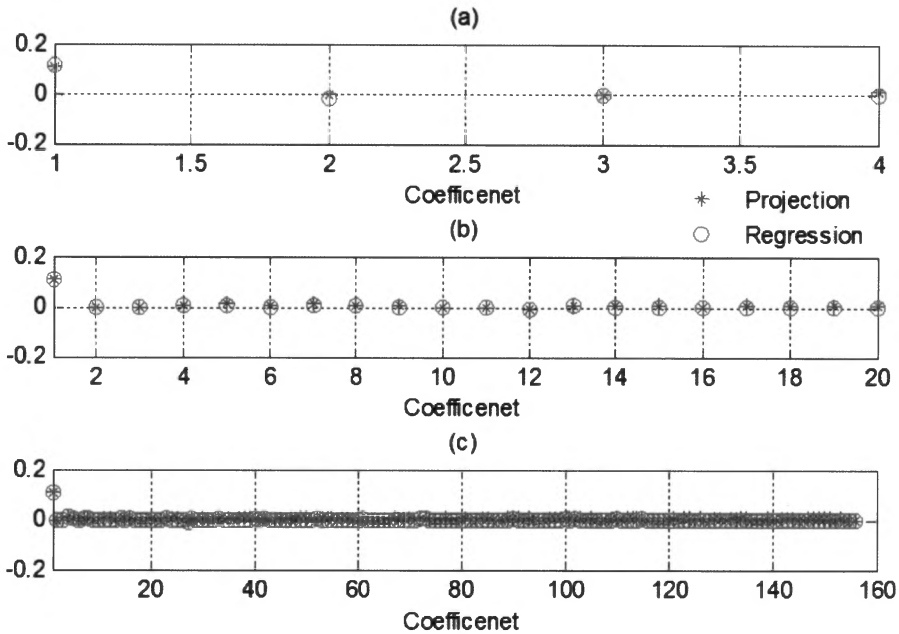

Figure 3-4 The coefficient calculated by the projection method and regression method.

The coefficients calculated by two methods are different, but the differences are very small, the first coefficient is much larger than the other coefficients for both projection method and regression method.

The mean and variance of the different polynomial chaos expansions are shown in Tab 3.2. The difference between the mean and variance calculated by polynomial chaos expansion and 50000 Monte Carlo simulations are also listed in the table.

Tab. 3 The mean value and variance of the different polynomial chaos expansions

Method	Projection (Quadrature)			Regression(LARS)		
Polynomial order	1	3	8	1	3	8
Number of sampling	7	83	2541	7	83	2541
Mean	0.1074	0.1056	0.1107	0.1160	0.1095	0.1093
Error of the mean (%)	1.79	3.51	1.3	6.06	0.13	0.06
Variance (10^{-4})	1.2393	4.4722	6.2859	2.2814	2.3921	2.5421
Error of the variance (%)	47.84	88.23	164.52	3.98	0.68	6.99

From Tab 3.2, the mean values for projection method are 0.1074, 0.1056 and 0.1107 with the corresponding error 1.79%, 3.51% and 1.3% when using first order, third order and eighth order polynomial chaos expansions. For regression method, the mean values are 0.1160, 0.1095 and 0.1093 with the corresponding error 6.06%, 0.13% and 0.06% when using first order, third order and eighth order polynomial chaos expansions. The performance of the regression method in mean is worse than projection method for first order polynomial chaos expansion. However, the error quickly reduced with increase the order for regression method. The error can be as small as 0.06% for eighth order polynomial chaos expansion using regression method, while the error for projection method with same order is 1.3%.

The variance for projection method are 1.2393×10^{-4}, 4.4722×10^{-4} and 6.2859×10^{-4} with the corresponding error 47.84%, 88.23% and 164.52% when using first order, third order and eighth order polynomial chaos expansions. For regression method, the variance are 2.2814×10^{-4}, 2.3921×10^{-4} and 2.5421×10^{-4} with the corresponding error 3.98%, 0.68% and 6.99% when using first order, third order and eighth order polynomial chaos expansions. The performance of the regression method in variance is much better than projection method especially for high order polynomial chaos expansions.

Tab. 3.4 The Sobol index for uncertainty variables

	order	Projection (Quadrature)			Regression(LARS)		
		m	*c*	*k*	*m*	*c*	*k*
First order	1	0.5755	0.0237	0.4008	0	0	1
	3	0.3210	0.1137	0.2963	0.3362	0.017	0.3127
	8	0.1507	0.1009	0.1186	0.3320	0.014	0.2415
Total	1	0.5755	0.0237	0.4008	0	0	1
	3	0.5883	0.1170	0.5643	0.6614	0.029	0.6439
	8	0.6621	0.4874	0.6551	0.7436	0.020	0.6531

Tab.3.5 The error for each Sobol index (%)

	order	Projection (Quadrature)			Regression(LARS)		
		m	*c*	*k*	*m*	*c*	*k*
First order	1	31.30	119.58	49.43	100	100	272.86
	3	26.77	952.64	10.46	23.29	53.46	16.60
	8	65.62	834.57	55.77	24.25	33.38	9.97
Total	1	19.01	31.75	36.96	100	100	57.28
	3	17.21	549.82	11.24	6.92	61.59	1.28
	8	6.82	2607.99	3.03	4.64	12.78	2.73

From Tab.4, the Sobol indexes for regression method are much better than projection method except for the first order polynomial chaos expansion.

In conclusion, the projection method is better than regression method for low order polynomial chaos expansion in mean and Sobol indices. However, the variance for regression method is much better than projection method. In high order, the regression is better than regression method in all indexes. Thus, the regression method is used to calculate the polynomial chaos expansion when DDE model contains time delay.

3.1.4 ORDER OF THE POLYNOMIAL CHAOS EXPANSION

The higher order polynomial chaos always get the better results, but it also means more calculation time and sampling numbers, so it is necessary to select the suitable degree to improve the efficiency. Then the order form 3 to 15 have been conducted to make the calculations. The results showed in Figure 3-5.

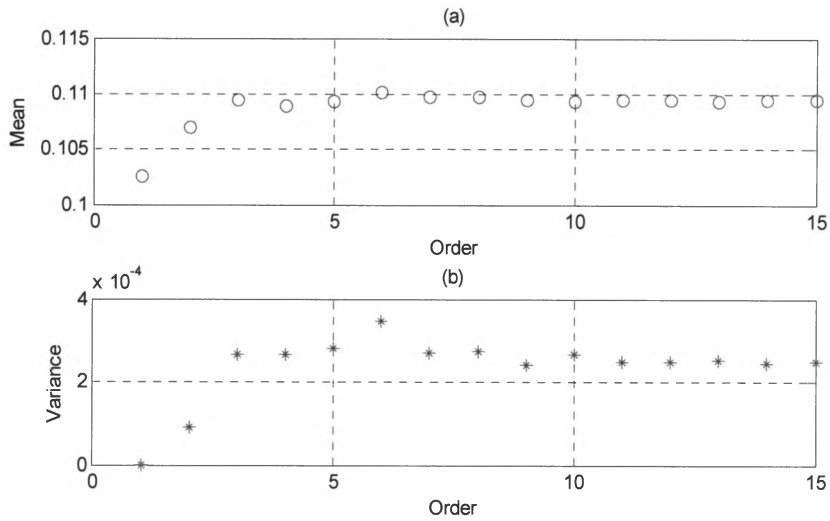

Figure 3-5 The performance of different order polynomial chaos for mean and variance of the maximum displacement.

It is obviously that both mean and variance convergence at third order, which are 0.1094 and 1.2393×10^{-4} respectively. Since polynomial chaos expansion is a sample based method, different sample points can lead to different results. Thus, the mean and variance for third order polynomial chaos expansion in this place has a little difference from the mean value and variance in Tab.2. The errors between the mean and variance calculated by third order polynomial and 50000 Monte Carlo simulations are 0% and 12.7%. Also, the Sobol indices are shown in Figure 3-6.

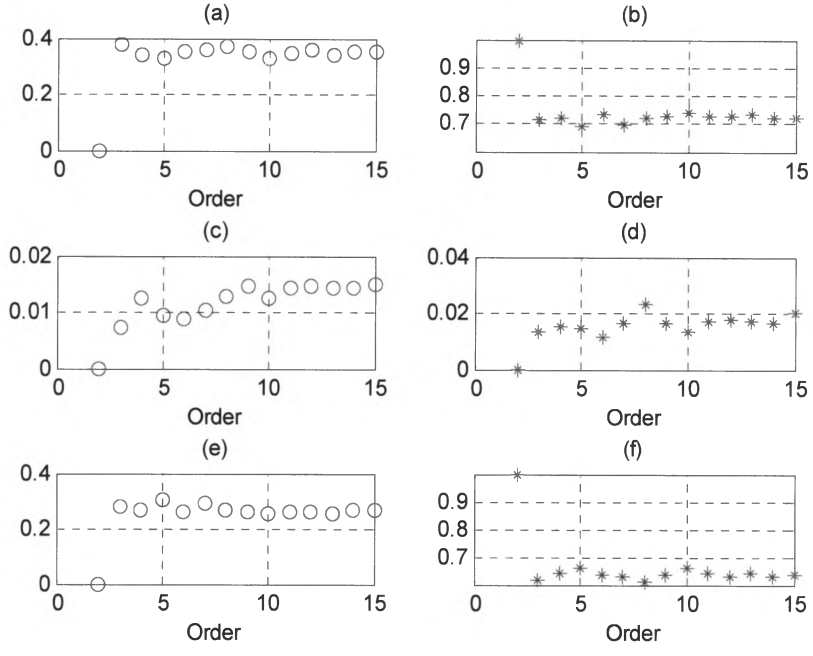

Figure 3-6 Sobol indices for random variables at different orders

Similar to mean and variance, the Sobol indexes are also convergence at third order polynomial. The first Sobol indexes for mass, damping and stiffness are 0.3755, 0.0073 and 0.2757 respectively for third order polynomial chaos expansion, which the corresponding errors are 14.33%, 47.95%, 2.80%. The total Sobol indices for mass, damping and stiffness are 0.7137, 0.0135 and 0.6143 respectively for third order polynomial chaos expansion, which the corresponding errors are 0.44%, 25.00%, 0.82%. Thus, the third polynomial chaos expansion is used to evaluate the influence of the delay in DDE models.

3.2 POLYNOMIAL CHAOS EXPANSION FOR SDOF SYSTEM WITH DELAY

3.2.1 THE COEFFICIENTS OF THE POLYNOMIAL CHAOS EXPANSION

Since the third order polynomial chaos expansion is used with regression method to calculate the influence of the time delay in DDE model when mass, damping and stiffness are random variables. And the coefficients can be calculated and shown in Figure 3-7. The time delay selected from 0.5ms to 5ms every 0.5ms.

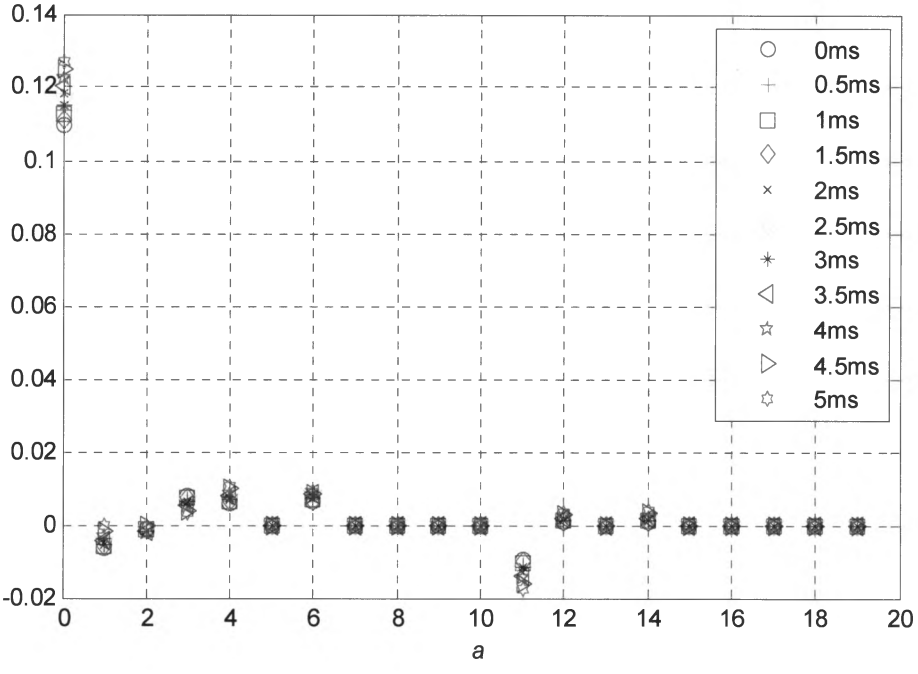

Figure 3-7 The coefficients of polynomial chaos under different time delay

The first coefficient for each polynomial chaos expansion represents the mean of the maximum displacement, while the summation square of rest coefficients represents the variance. From Fig.3-7, the mean and variance of the maximum displacement vary with time delay.

3.2.2 DELAY EFFECT ON THE MEAN OF THE MAXIMUM DISPLACEMENT

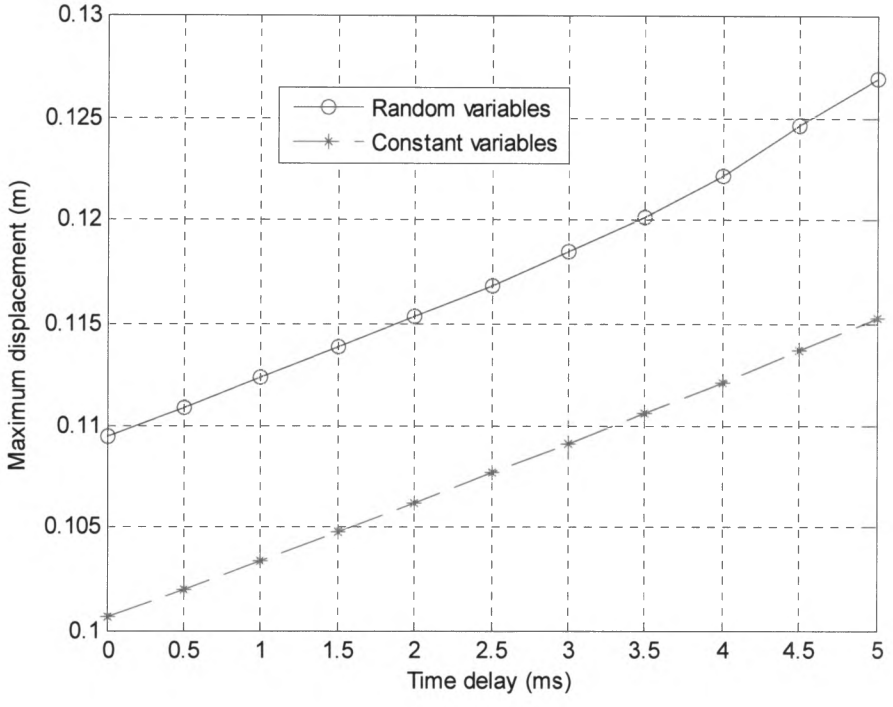

Figure 3-8 Relationship between time delay and the mean of maximum displacement

The relationship between the mean of the maximum displacement and time delay for random variables is shown in Figure 3-8. Meanwhile, the maximum displacements for constant mass, damping and stiffness when equal to the mean are also presented in the figure. For random variable case, the maximum displacement increase with time delay linearly with two different slopes. When the time delay is less than 3.5ms, the slope is 0.003m/ms, then the slope increases to 0.004m/ms after 3.5ms. When compared with the results for constant variables, the maximum displacements for random variables are about 10% larger, which is consistence with 50000 Monte Carlo simulations. The difference between the maximum displacements for random variables and constant variables grows with time delay, which shows the requirement for uncertainty quantification again.

3.3.3 DELAY EFFECT ON THE VARIANCE OF THE MAXIMUM DISPLACEMENT

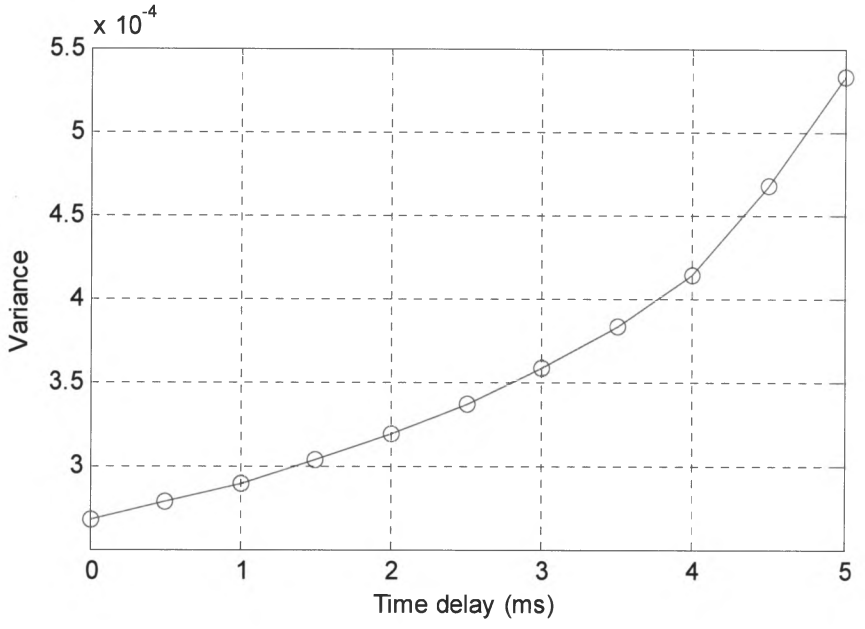

Figure 3-9 Relationship between time delay and the variance of maximum displacement

The relationship between the variance of the maximum displacement and time delay for random variables is shown in Figure 3-9. From Figure 3-9, it can be recognized that the variance of the maximum displacement grow with time delay exponentially. When DDE model contains random variables, the time delay could enhance the uncertainty of the model output. The variance of the maximum displacement is more than twice when time delay is 5ms than no delay case.

3.3.4 DELAY EFFECT ON SOBOL INDICES OF RANDOM VARIABLES

The relationships between the Sobol indices of the random variables and time delay are shown in Figure 3-10.

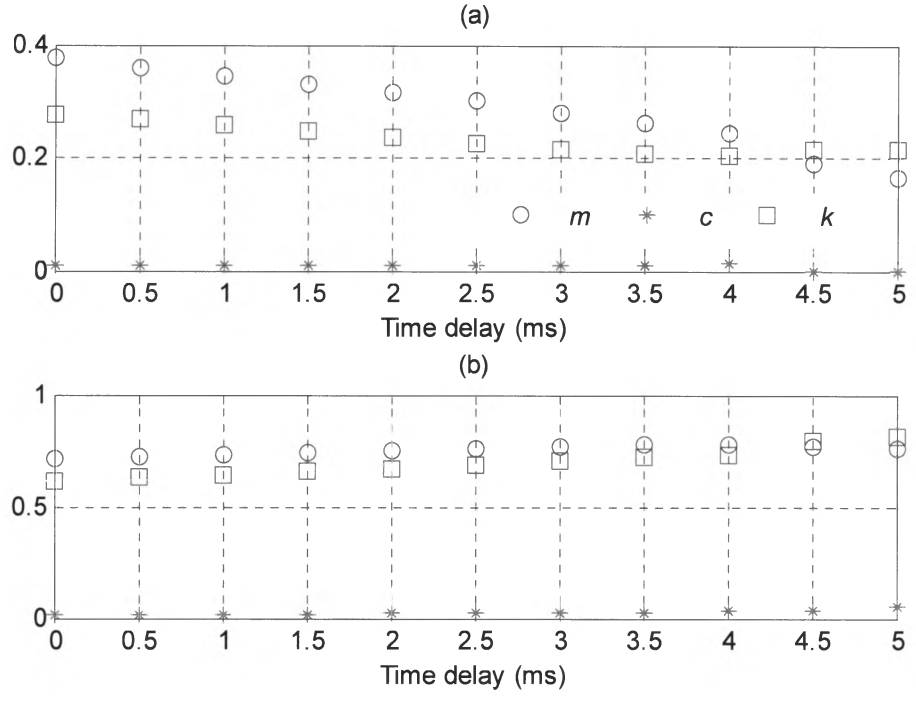

Figure 3-10 Relationship between time delay and Sobol indices of the random variables for (a) First order Sobol indices and (b) Total Sobol indices

From the figure 3-10, the first Sobol indices for all mass, damping and stiffness decrease with the time delay, while the total Sobol indices increase with time delay for all variables, however, first Sobol index always represents the single parameter influence the output while the total Sobol index represents influence of one parameter combined with other parameters on the total output. So, this way, it means time delay can increase the coupling effect of the random variables while the influence of single random variable will decrease with time delay increase.

Besides, the most important parameter affect the variance of the maximum displacement has changed from mass to stiffness after 4.5ms. Thus, time delay can change the variable which has the most influence on the variance of the maximum displacement in DDE model.

CHARPTER IV:

DELAY EFFECT ON TWO-DEGREES OF FREEDOM (TDOF) SYSTEM

4.1 TWO-DEGREES-OF-FREEDOM (TDOF) SYSTEM

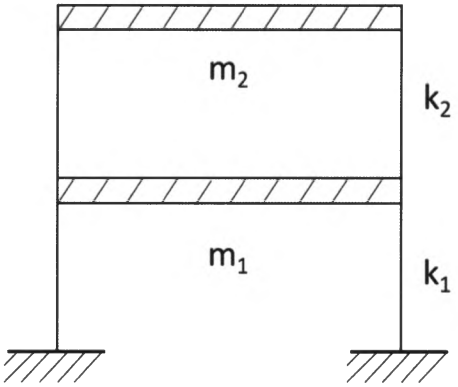

Figure 4-1 Two-degrees of freedom system

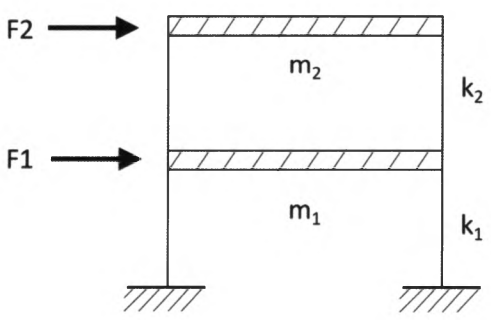

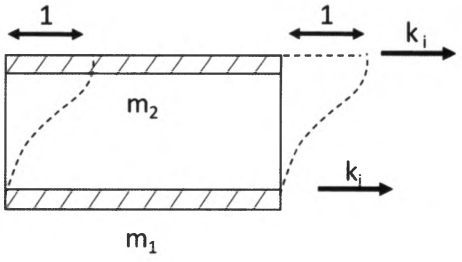

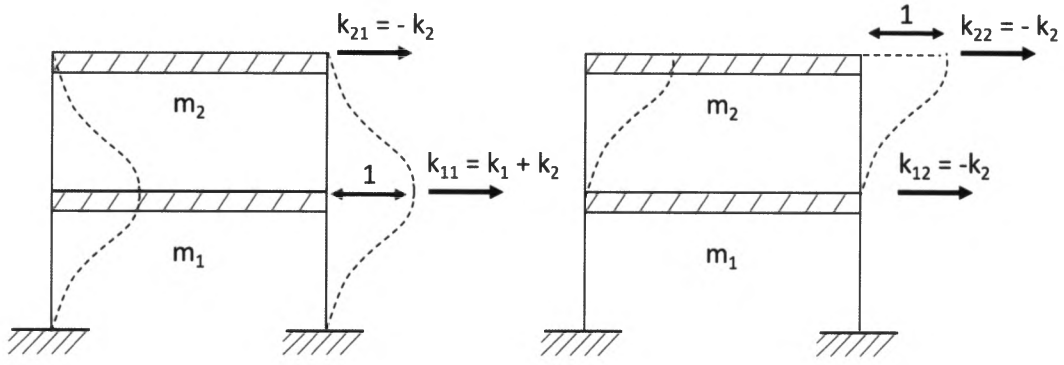

Figure 4-1 shows schematics of a two-story-of-freedom structure with the m_1 and m_2, stiffness of k_1 & k_2 and damping ratios of c_1& c_2 for the first floor and second floor.

4.2 EQUATION OF MONTION FOR TDOF SYSTEM

$$[m]\cdot\ddot{x}(t)+[c]\cdot\dot{x}(t)+[k]\cdot x(t)=F(t) \tag{4-1}$$

Where [m], [c] and [k] are mass matrices, damping matrices and stiffness matrices, x (t) is the displacement vector and F (t) is the excitation force. And $\ddot{x}(t)=\begin{pmatrix}\ddot{x}_1(t)\\ \ddot{x}_2(t)\end{pmatrix}$, $\dot{x}(t)=\begin{pmatrix}\dot{x}_1(t)\\ \dot{x}_2(t)\end{pmatrix}$, $x(t)=\begin{pmatrix}x_1(t)\\ x_2(t)\end{pmatrix}$ and $F(t)=\begin{pmatrix}F_1(t)\\ F_2(t)\end{pmatrix}$.

From the Figure 2-2, the [m], [c] and [k] can be determined:

$$[m]=\begin{bmatrix}m_1 & 0\\ 0 & m_2\end{bmatrix} \qquad [c]=\begin{bmatrix}c_1+c_2 & -c_2\\ -c_2 & c_2\end{bmatrix} \qquad [k]=\begin{bmatrix}k_1+k_2 & -k_2\\ -k_2 & k_2\end{bmatrix} \tag{4-2}$$

So the equation can be written as:

$$\begin{bmatrix} m_1 & 0 \\ 0 & m_2 \end{bmatrix} \cdot \begin{Bmatrix} \ddot{x}_1(t) \\ \ddot{x}_2(t) \end{Bmatrix} + \begin{bmatrix} c_1+c_2 & -c_2 \\ -c_2 & c_2 \end{bmatrix} \cdot \begin{Bmatrix} \dot{x}_1(t) \\ \dot{x}_2(t) \end{Bmatrix} + \begin{bmatrix} k_1+k_2 & -k_2 \\ -k_2 & k_2 \end{bmatrix} \cdot \begin{Bmatrix} x_1(t) \\ x_2(t) \end{Bmatrix} = \begin{Bmatrix} F_1(t) \\ F_2(t) \end{Bmatrix} \quad (4\text{-}3)$$

Rewrite the equations as below:

$$\begin{aligned} m_1 \cdot \ddot{x}_1(t) + (c_1+c_2) \cdot \dot{x}_1(t) - c_2 \cdot \dot{x}_2(t) + (k_1+k_2) \cdot x_1(t) - k_2 \cdot x_2(t) = F_1(t) \\ m_2 \cdot \ddot{x}_2(t) - c_2 \cdot \dot{x}_1(t) + c_2 \cdot \dot{x}_2(t) - k_2 \cdot x_1(t) + k_2 \cdot x_2(t) = F_2(t) \end{aligned} \quad (4\text{-}4)$$

As the Single Degree of Freedom System, time delays exist in the response of servo-hydraulic actuators, so the equations of the two-degrees of freedom system should be revised as (where τ is the time delay):

$$\begin{aligned} m_1 \cdot \ddot{x}_1(t) + (c_1+c_2) \cdot \dot{x}_1(t) - c_2 \cdot \dot{x}_2(t) + (k_1+k_2) \cdot x_1(t-\tau) - k_2 \cdot x_2(t-\tau) = F_1(t) \\ m_2 \cdot \ddot{x}_2(t) - c_2 \cdot \dot{x}_1(t) + c_2 \cdot \dot{x}_2(t) - k_2 \cdot x_1(t-\tau) + k_2 \cdot x_2(t-\tau) = F_2(t) \end{aligned} \quad (4\text{-}5)$$

4.3 SIMULINK MODEL OF TDOF SYSTEM

Based on the Equation (4-5), the substructure system can be created as:

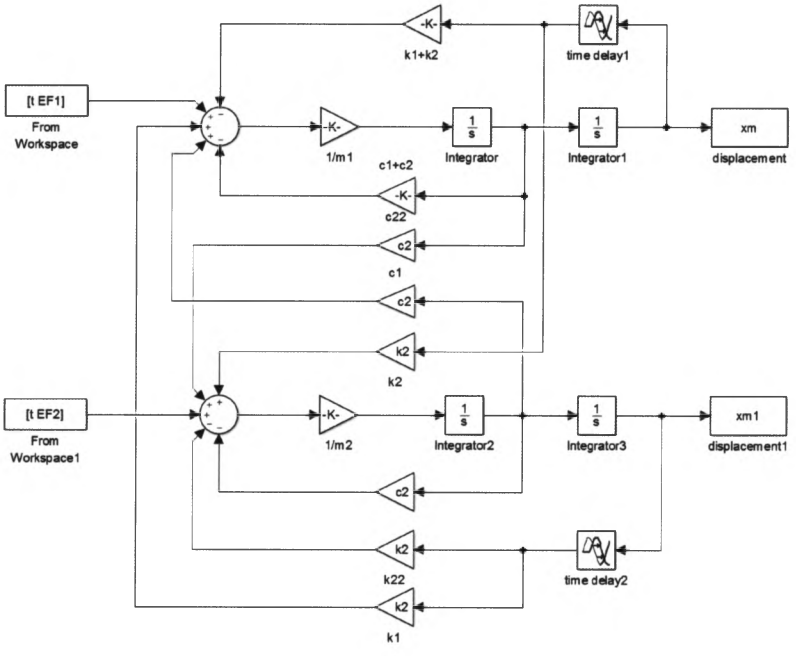

Figure 4-3 Block diagram representation for Two-degrees of freedom system

4.4 METHODS TO DETERMINE THE COEFFICIENTS AND ORDERS OF TDOF SYSTEM.

The Sparse-favoring Least-square minimization LARS is conducted to calculate the coefficients and it can be enabled similarly to OLS.

In this method, LARS allows for degree-adaptive calculation of the PCE coefficients: if any array of possible degrees is given, the degree with the lowest Leave-One-Out cross-validation error (LOO error) is automatically selected, the range of degree is from 3 to 15 in this study.

And in general, sparse PCE requires a vastly inferior number of samples to properly coverage w.r.t. to both quadrature and OLS and in this analysis, the sampling numbers are selected as 400.

4.5 DELAY EFFECT ON THE MEAN OF THE MAXIMUM DISPLACEMENT

Since this two-degree of freedom system, there are two different time delays exists in two stories and their stiffness should also be different. Both time delays selected from 0.001 to 0. 01 every 0.001, the stiffness of the first floor is k1 and k2 for the second story, the ratio of k2/k1 selected from 1.2 to 1.4 every 0.1.The result of delay effect on mean of maximum displacement showed in Figure below.

For the first story:

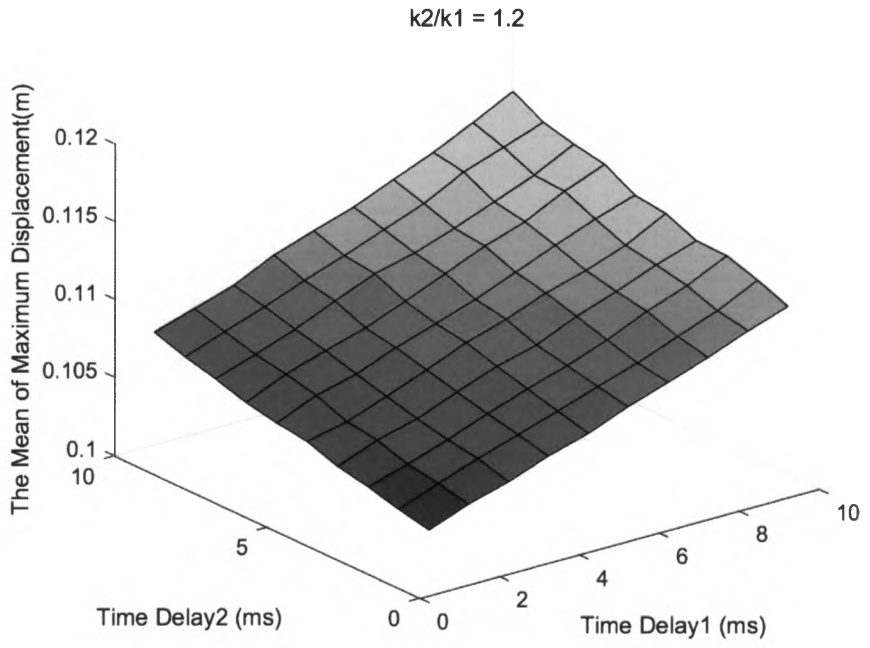

Figure 4-4 The mean of the maximum displacement under different time delays when k2/k1 = 1.2

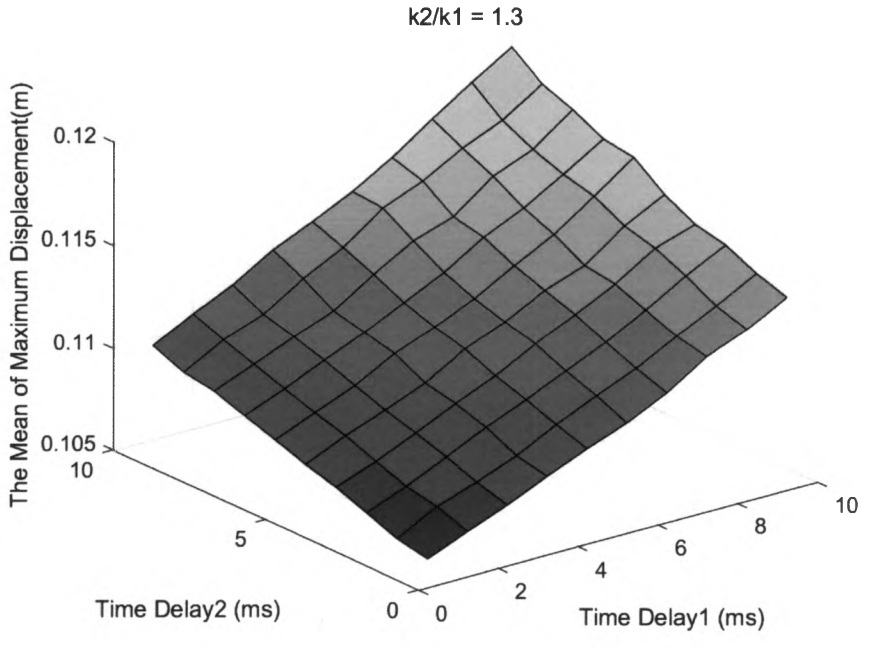

Figure 4-5 The mean of the maximum displacement under different time delays when k2/k1 = 1.3

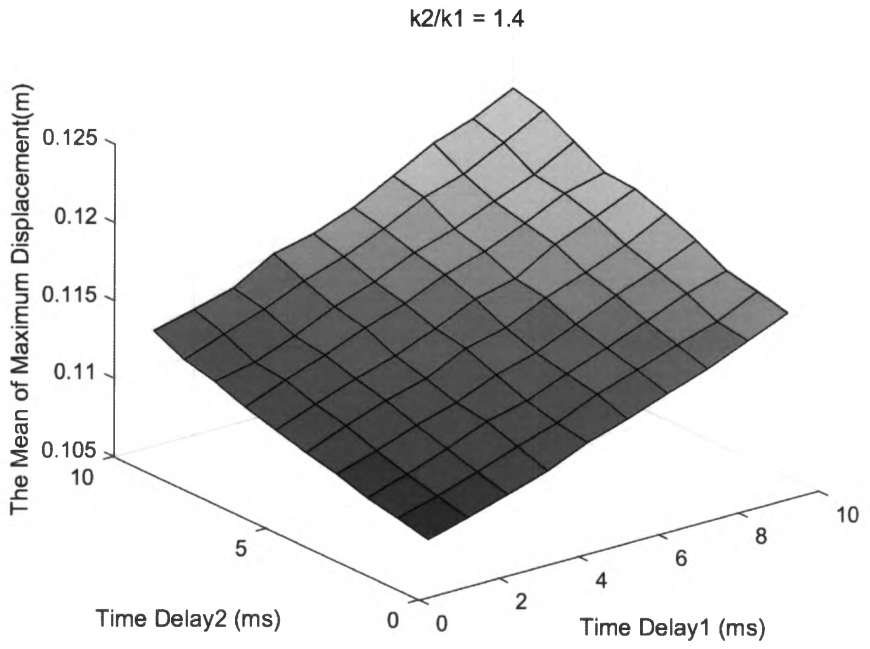

Figure 4-6 The mean of the maximum displacement under different time delays when k2/k1 = 1.4

For the second floor:

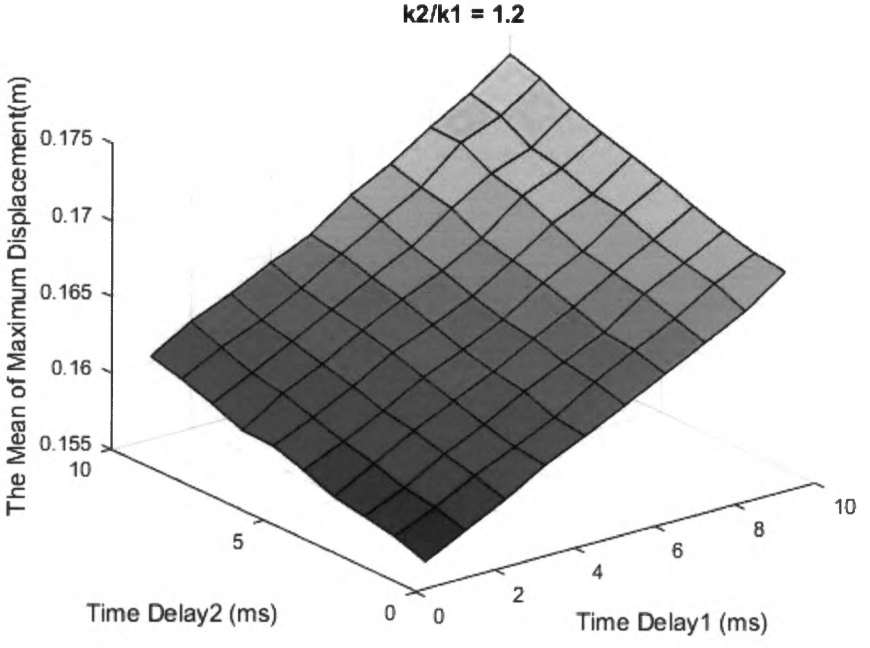

Figure 4-7 The mean of the maximum displacement under different time delays when k2/k1 = 1.2

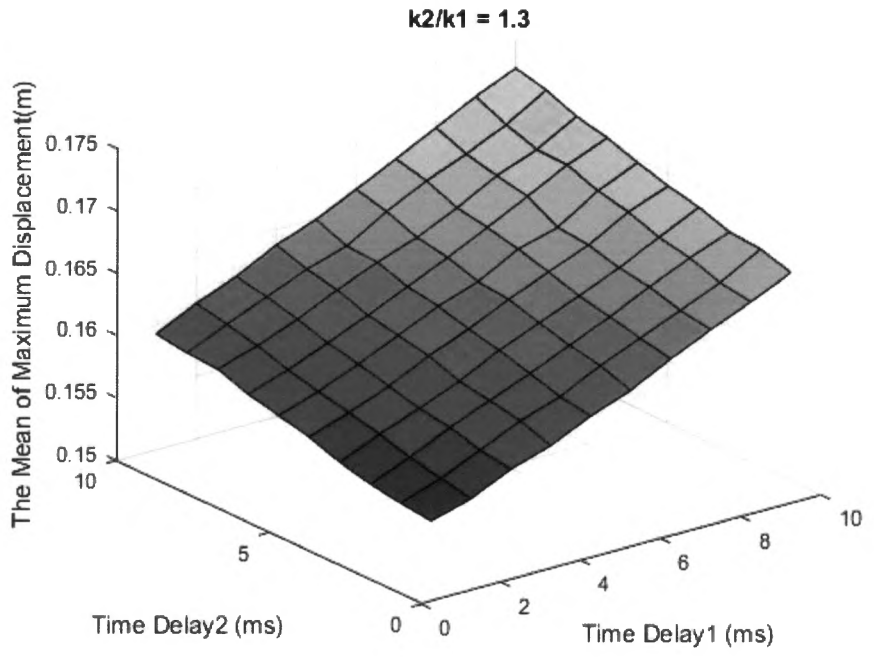

Figure 4-8 The mean of the maximum displacement under different time delays when k2/k1 = 1.3

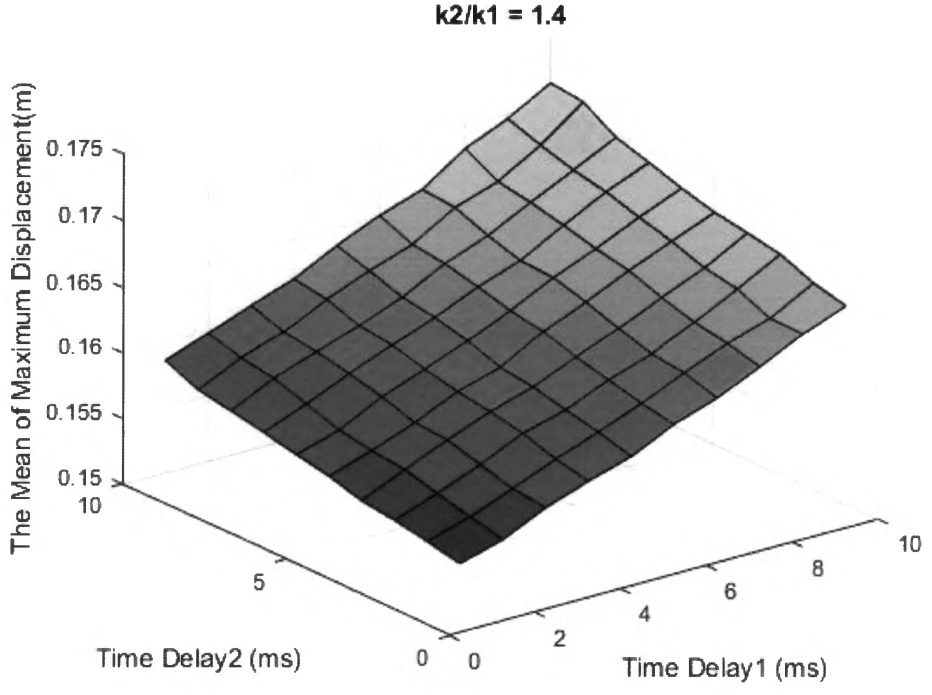

Figure 4-9 The mean of the maximum displacement under different time delays when k2/k1 = 1.4

The relationship between the mean of the maximum displacement and time delay for random variables is shown in Figure 4-4 – Figure 4-9. Under the same ratio of k2/k1, it obviously shows that the value of the mean maximum displacement will get larger when increase time delays. Compared with different ratio cases, the values of the mean maximum displacement are 0.1090, 0.1128, 0.1163, 0.1193, 0.1216, and 0.1236 for the first story. This means the peak value of the mean maximum displacement will also increase with the ratio. Thus, both the ratio of k2/k1 and time delay will affect the value of the mean maximum displacement.

Also, the relationship between the mean maximum displacement and time delay when time delay 1 equal time delay 2 has been discussed. The results shown in Figure 4-10-Figure 4-11.

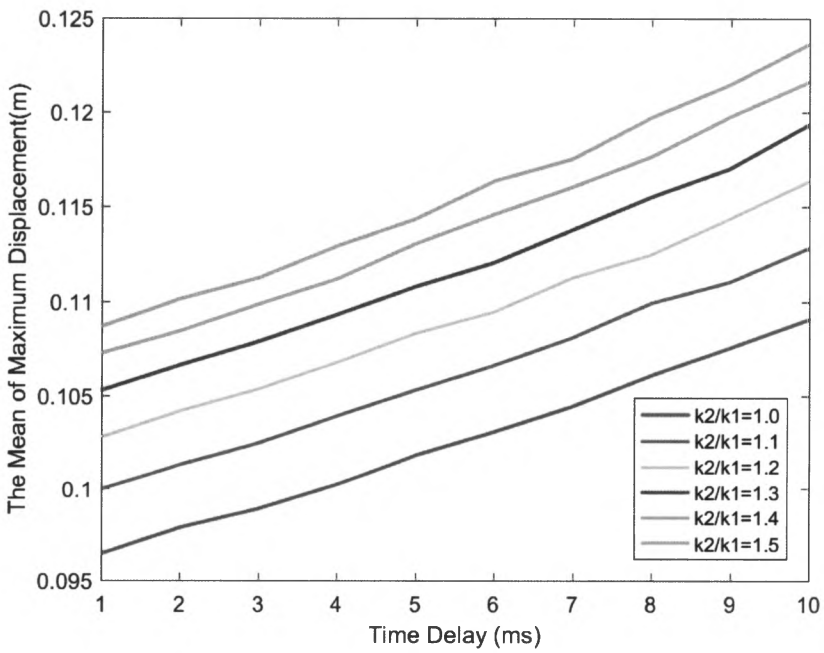

Figure 4-10 The relationship between the mean of maximum displacement under the same time delay for 1st story

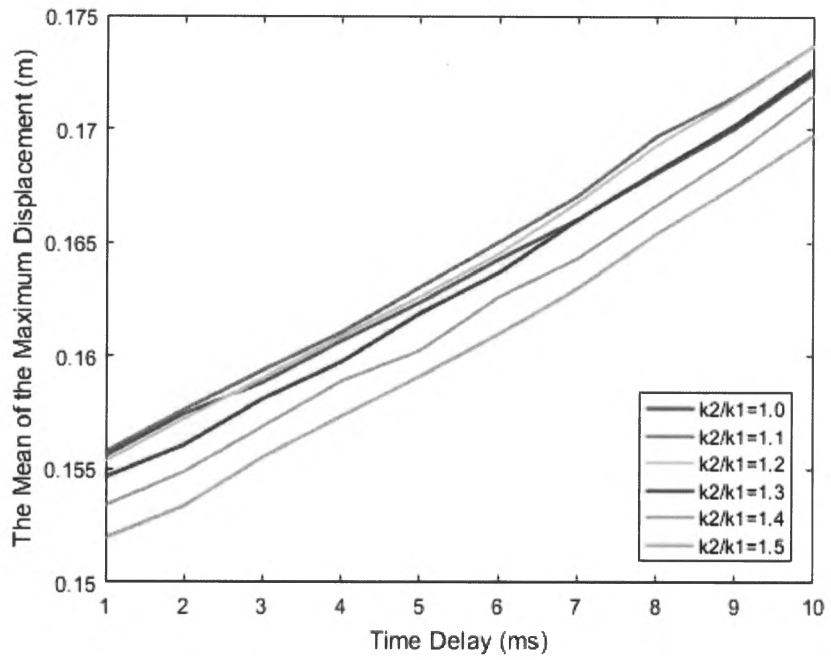

Figure 4-11 The relationship between the mean of maximum displacement under the same time delay for 2nd story

Similar to the different time delay case, the results also the time delays will increase the mean value of the maximum displacement, even when the time delay 1 equal time delay 2 and the time delays have more influence on the second floor than the first floor due to the mean values of the maximum displacement. The ratio of k2/k1 has affected the mean values of the first floor while for the second floor, the values almost the same.

4.5 DELAY EFFECT ON THE VARIANCE OF THE MAXIMUM DISPLACEMENT

Different to the SDOF system, the delay effect on variance of the maximum displacement has been non-linearly but from the results, it seems still has obvious change trend that the variance of the maximum displacement go up with the increase of the time delays and the value arrived at the moment of the largest combination of two time delays.

For the first floor:

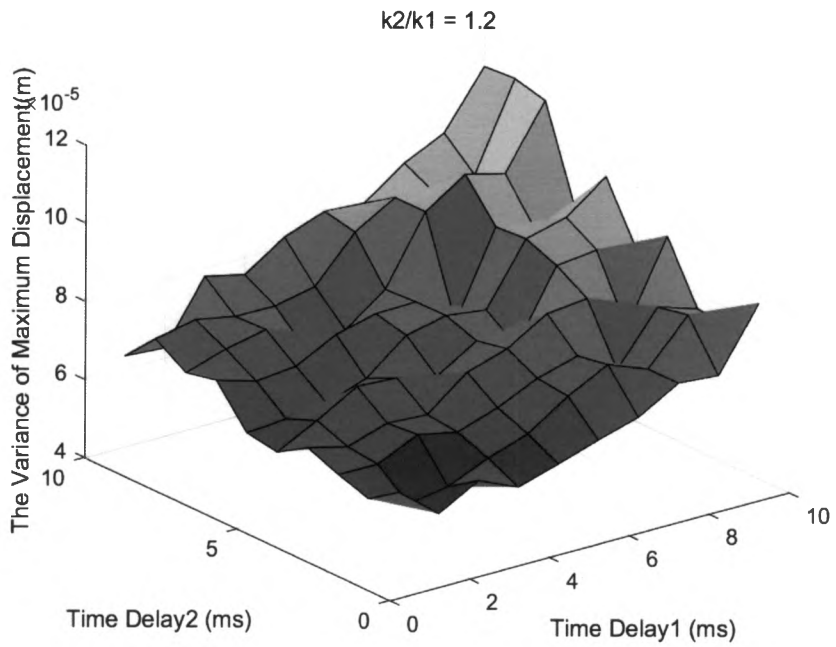

Figure 4-12 The variance of the maximum displacement under different time delays when k2/k1 = 1.2

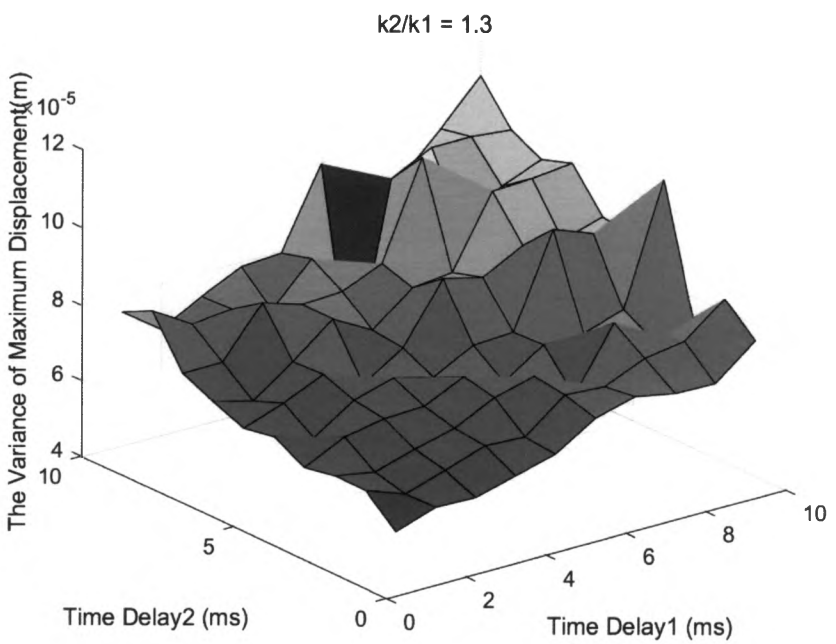

Figure 4-13 The variance of the maximum displacement under different time delays when k2/k1 = 1.3

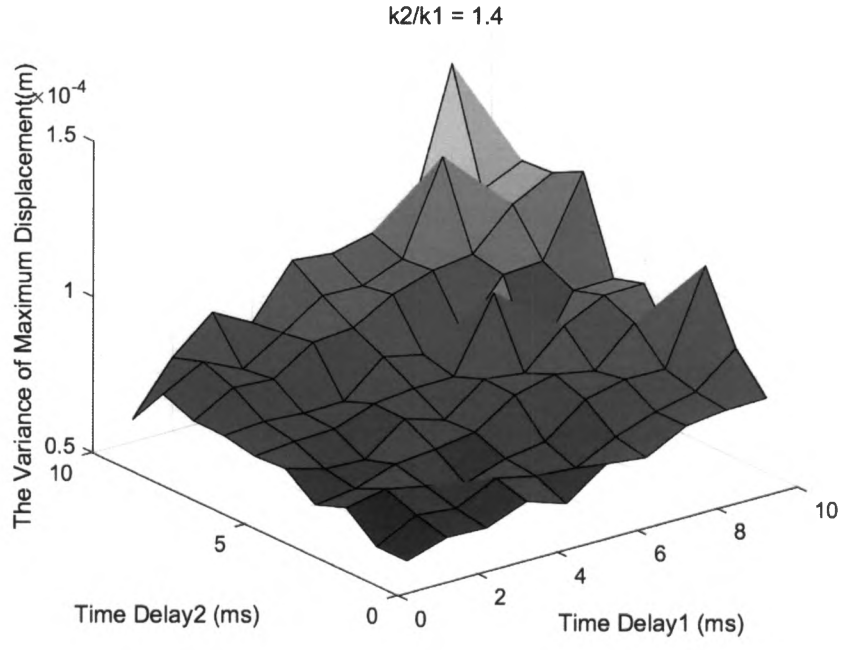

Figure 4-14 The variance of the maximum displacement under different time delays when k2/k1 = 1.4

For the second floor:

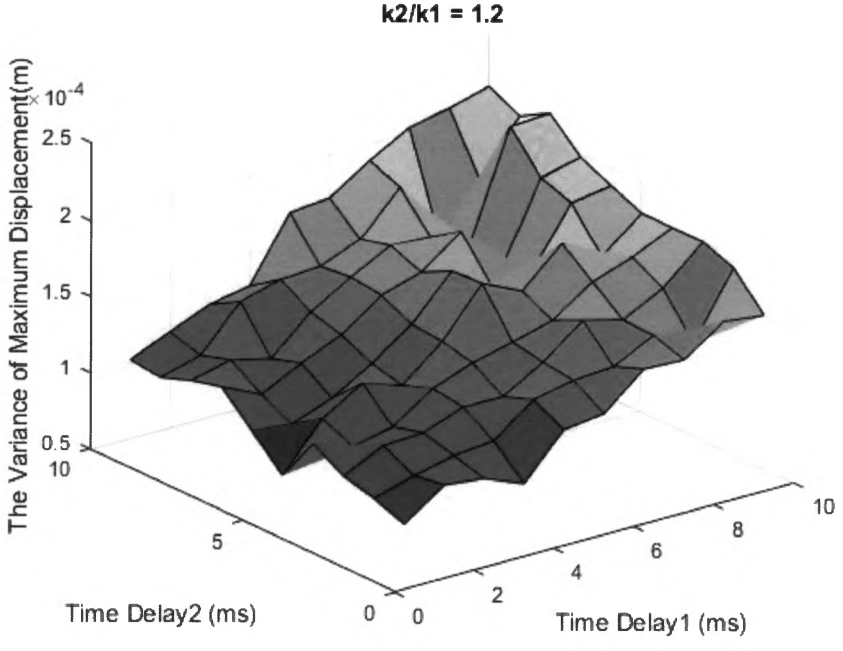

Figure 4-15 The variance of the maximum displacement under different time delays when k2/k1 = 1.2

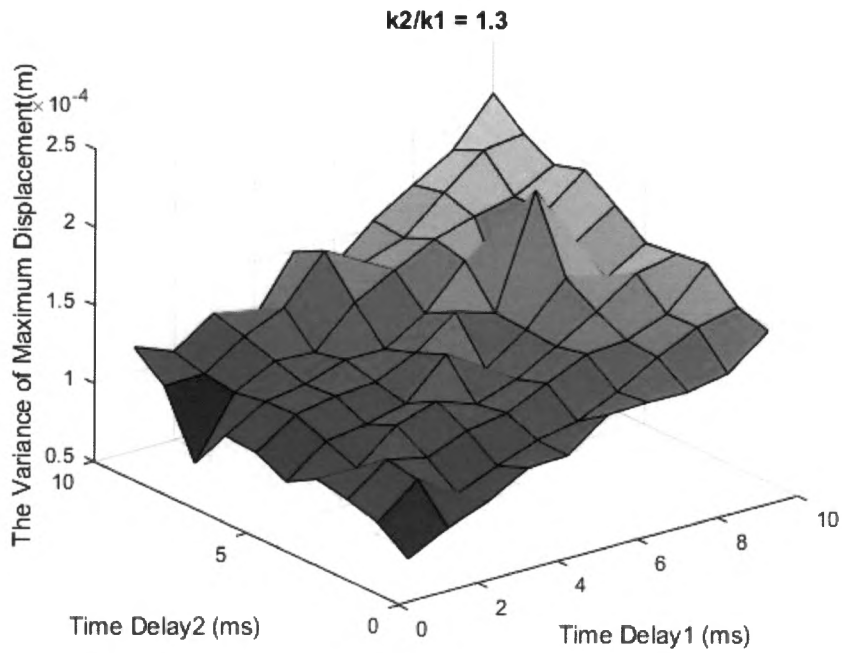

Figure 4-16 The variance of the maximum displacement under different time delays when k2/k1 = 1.3

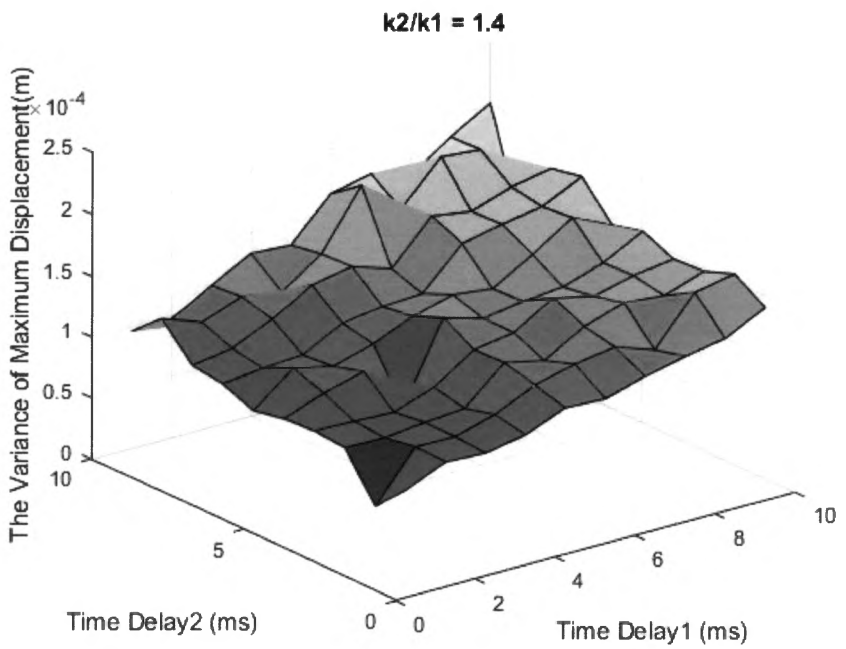

Figure 4-17 The variance of the maximum displacement under different time delays when k2/k1 = 1.4

4.6 DELAY EFFECT ON SOBOL INDICIES OF RANDOM VARIABLES

In this study, there are three random variables exist which named stiffness ratio, time delay 1 and time delay2 and six random variables ($m_1, c_1, k_1, m_2, c_2, k_2$) chose as PCE inputs. Thus, 1000 set of First Sobol indices and Total Sobol indices will be created as the result of Sobol Analysis. By this way, it is important to select several meaningful data to do the analysis.

When k2/k1 = 1.0, time delay 1 = 0.001s, time delay 2 = 0.001s to 0.01s, the results shown in Figure 4-18 – Figure 4-19.

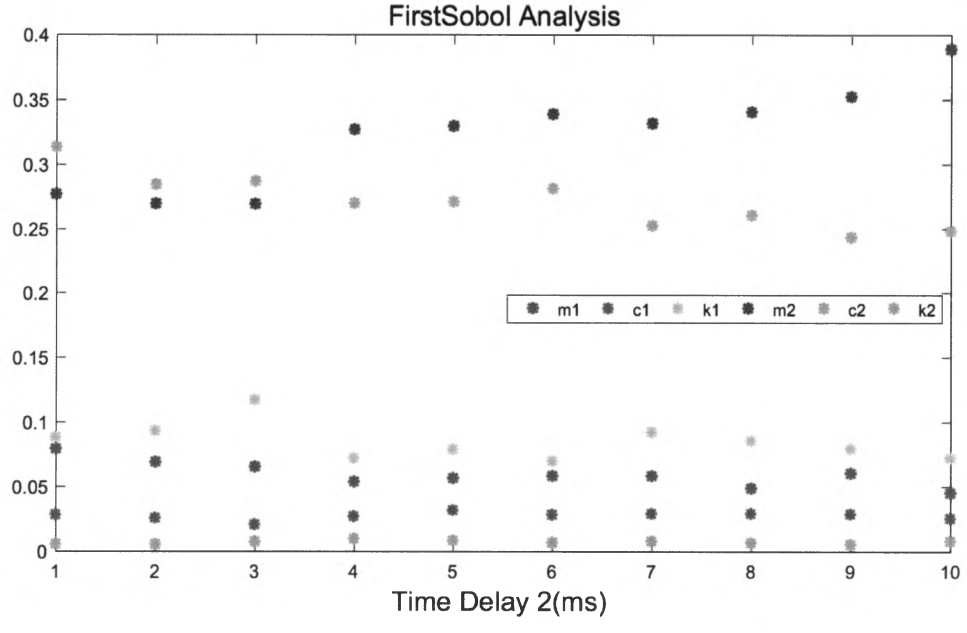

Figure 4-18 First Sobol indices for delay effect on random variables when time delay 2 = 0.001 to 0.01s

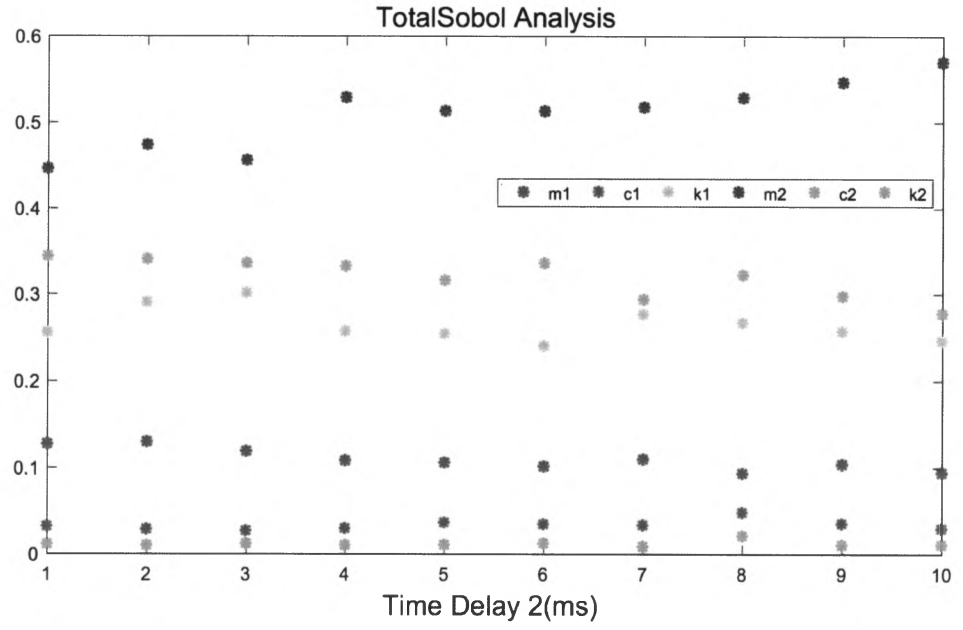

Figure 4-19 Total Sobol indices for delay effect on random variables when time delay 2 = 0.001 to 0.01s

When k2/k1 = 1.0, time delay 1 = 0.001 to 0.01s, time delay 2 = 0.001s, the results shown in Figure 4-20 – Figure 4-21.

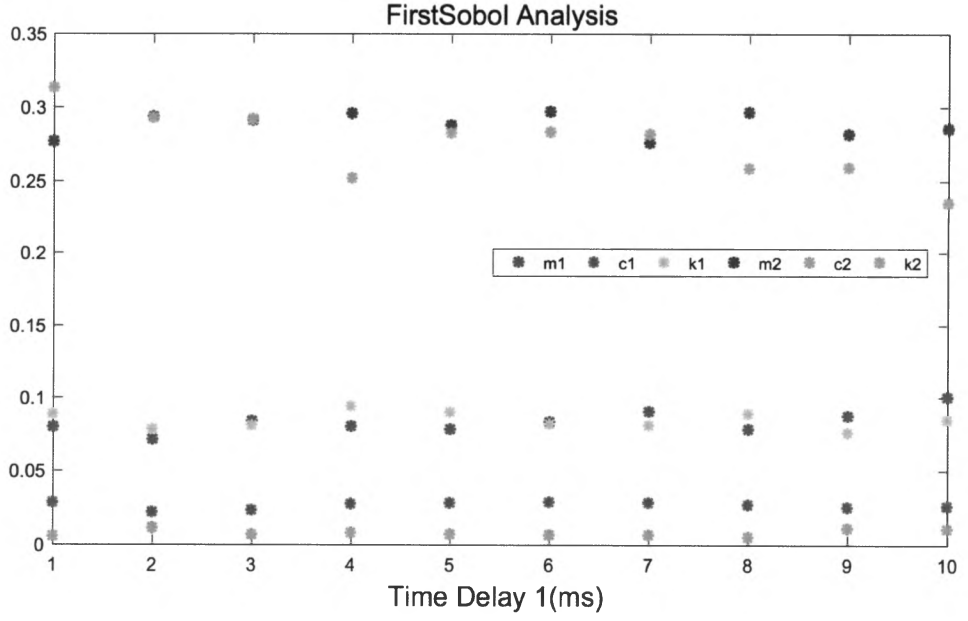

Figure 4-20 First Sobol indices for delay effect on random variables when time delay 1 = 0.001 to 0.01s

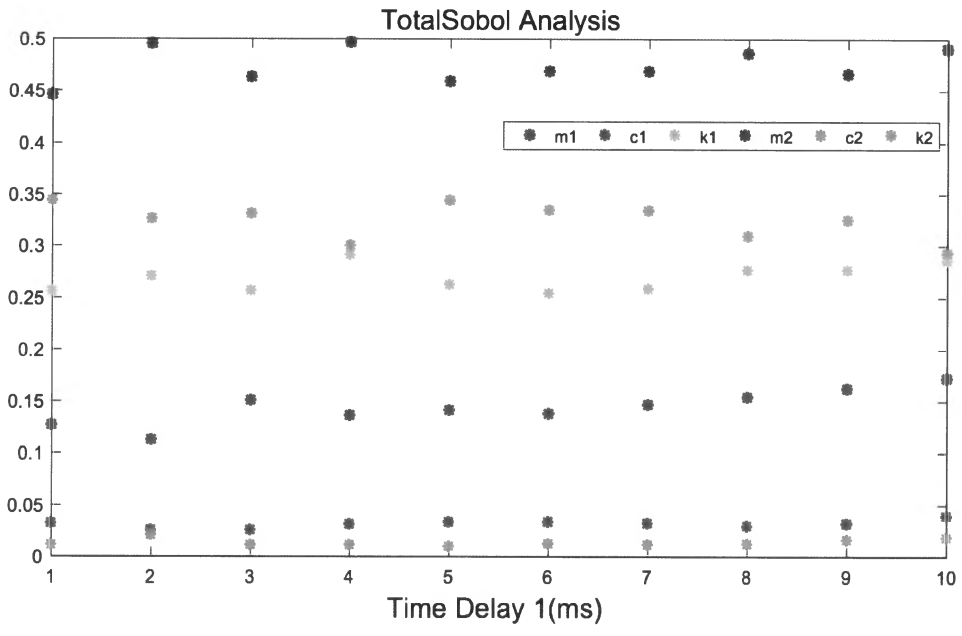

Figure 4-21 Total Sobol indices for delay effect on random variables when time delay 1 = 0.001 to 0.01s

When k2/k1 = 1.0, both time delay 1and time delay 2 = 0.001 to 0.01s, the results shown in Figure 4-22 – Figure 4-23.

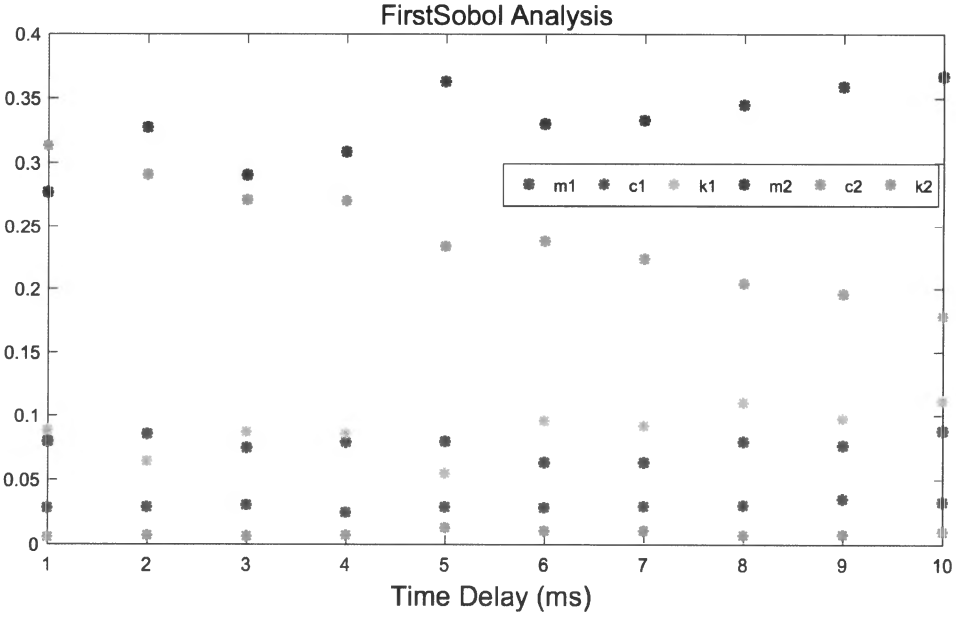

Figure 4-22 First Sobol indices for delay effect on random variables when time delay 2&time delay 1 = 0.001 to 0.01s

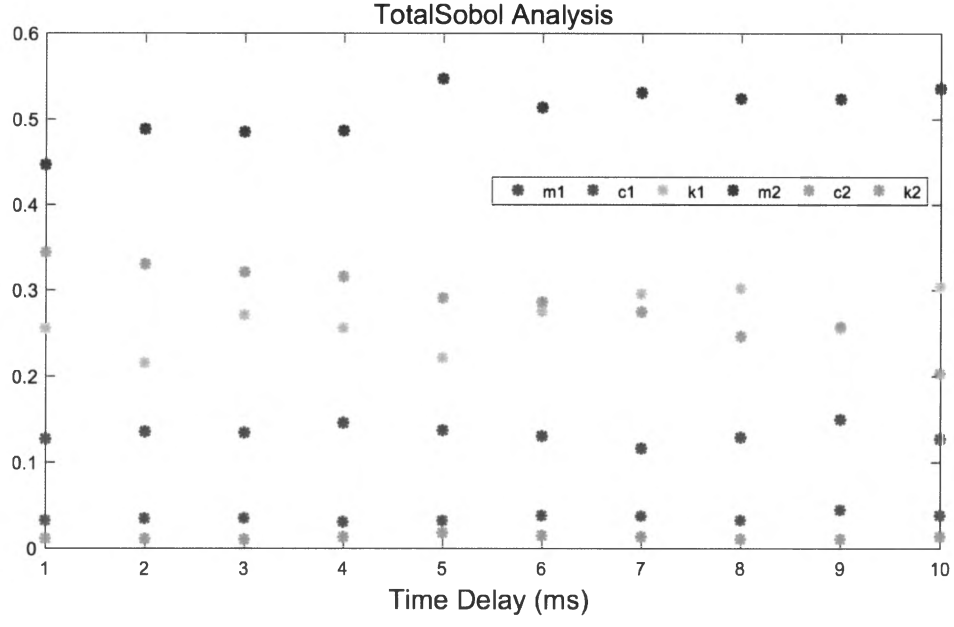

Figure 4-23 Total Sobol indices for delay effect on random variables when time delay 2&time delay 1 = 0.001 to 0.01s

The relationships between the Sobol indices of the random variables and time delay are shown in Figure 4-11-Figure 4-16. Similar to the SDOF case, both the first Sobol indices and total Sobol indices for all mass, damping and stiffness vary with the time delay. But for the first Sobol indices part, the m_1, c_1, k_1, c_2 vary in a very small range which can be ignored, while the most important parameter influence the output variance has changed from the k_2 to m_2. Different to the first Sobol indices, the total Sobol indices show that the most important parameter always is the m_2, and value of k_1 exceeded k_2 after time delay increase.

Thus, for the TDOF system, both the first Sobol indices and total Sobol indices have no linearly behavior for single parameters, but the rank of the most influence parameter will make changes with the time delays increase and the random variables of second story always have much more influence than the parameter of first story.

CHAPTER V:

SUMMARY AND CONCLUSION

Both numerical substructure and experimental substructure exists uncertainties in real-time hybrid simulation. The uncertainties may results in different structure responses even for the same model and control in real-time hybrid simulation. In this paper, DDE model with random variables is selected to study the effect of the delay when model contains uncertainty parameters. Polynomial chaos expansion is used to build the relationship between uncertainty variables and the maximum displacement.. Based on the assumptions and limitations of this paper, conclusions are drawn as follows

1 The mean of the maximum displacement when model contains random variables does not necessarily equal to the maximum displacement when random variables equal to their mean values. This lead to the requirement for uncertainty qualification when model contains random variables.

2 For DDE model, third order polynomial chaos expansion using regression method (LARS) is most suitable to build the metamodel between of the maximum displacement and random variables.

3 For SDOF system, the mean and variance of the maximum displacement increase with time delay linearly and exponentially, respectively. The difference between the mean of the maximum displacement and the maximum displacement when random variables equal to their mean values grows with time delay. For TDOF system, both the ratio of k2/k1 and time delay will affect the value of the mean maximum displacement. But for the variance part, the delay effect on variance of the maximum displacement has been non-

linearly but from the results, it seems still has obvious change trend that the variance of the maximum displacement go up with the increase of the time delays

4 Time delay can change the variable which has the most influence on the variance of the maximum displacement in both SDOF system and TDOF system

REFERENCES

1 Liu YN (2013), "Non-Intrusive Methods for Probabilistic Uncertainty Quantification and Global Sensitivity Analysis in Nonlinear Stochastic Phenomena", the Florida State University, ProQuest Dissertations Publishing, publication number: 3612453.

2 Christopher Z., Mooney (1997), "Monte Carlo Simulation", Vol. 116. Sage Publications.

3 Rubinstein R.Y., Kroese D.P. (2007), "Simulation and the Monte Carlo Method", John Wiley & Sons, Inc., Hoboken, NJ.

4 Helton J. C. and Davis F.J. (2003), "Latin hypercube sampling and the propagation of uncertainty in analyses of complex systems", Reliability Engineering and System Safety, Volume 81, Issue 1, Pages 23-69.

5 Niederreiter H. et al. (2010), "Quasi – Monte Carlo Simulation", Journal of Computational and Applied Mathematics, 2010.

6 Pettersson, Mass Per, et al. (2015), "Polynomial Chaos Methods for Hyperbolic Partial Differential Equations: Numerical Techniques for Fluid Dynamics Problems in the Presence of Uncertainties", Computer Methods in Applied Mechanics and Engineering, Springer.

7 Phoon K. K., Huang S. P. and Quek S. T (2002) ,"Simulation of second-order processes using Karhunen–Loeve expansion" Computer & Science 80.12.

8 Norbert W., (1938), "The homogeneous chaos." American Journal of Mathmatics.

9 Ernst O.G. et al. (2010), "On the Convergence of Generalized Polynomial Chaos Expansions", LMS Durham Symposium: Numerical Analysis of Multiscale Problems, 2010

10 Zheng M.D., Wan X.L. and Karniadakis K.G (2015), "An Adaptive Multi-Element Generalized Polynomial Chaos Method for Stochastic Differential Equations", Applied Numerical Mathematics.

11 Crestaux T. et al. (2009), "Polynomial chaos expansion for sensitivity", Reliability Engineering and System Safety.

12 Chen C, Ricles J.M, Marullo T.M. and Mercan (2009). "Real-time hybrid testing using the unconditionally stable explicit CR integration algorithm." Earthquake Engineering and Structural Dynamics 38:23-44.

13 Chen C, and Ricles J.M. (2008), "Stability analysis of SDOF real - time hybrid testing systems with explicit integration algorithms and actuator delay." *Earthquake Engineering & Structural Dynamics* 37.4: 597-613.

14 Chen C, and Ricles J.M. (2010), "Tracking Error-Based Servo hydraulic Actuator Adaptive Compensation for Real-Time Hybrid Simulation". Journal of Structral Engineering 136(4), 432-440.

15 Houriuchi T. et al. (1999), "Real-Time hybrid experimental system with actuator delay compensation and its application to a piping system with energy absorber." Earthquake Engineering & Structural Dynamics 28.10: 1121-1141.

16 Carrion J.E. and Spender B.F. (2006), "Real-Time hybrid testing using model-based delay compensation." Proceedings of the 4th International Conference on Earthquake Engineering. Vol.299.